Advances in Mechanics
Volume 9, Issue 3, 2021
Page 1215-1231

Analysis Of Heat Transfer With Natural Convection Of Non-Newtonian Fluid Inside An Enclosure With The Hot Obstacle

Zainab M. Agool[1], Rafel H. Hameed [2]

[1, 2] College of Engineering- Mechanical Engineering Department- University of Babylon- Babylon City- Hilla
(E-mail: Zainab.hassan4333@student.uobabylon.edu.iq)
(E-mail: eng.rafel.hekmat@uobabylon.edu.iq)

***Article history**:Received 07 July 2021 Revised 18 August 2021 Accepted 02 September 2021*

Abstract

The Non-Newtonian natural convection heat transfer in the enclosure of hot obstacles has been studied numerically and validated successfully. The streamlines, velocity contours, and heat transfer analysis have been included in the present investigation for various aspect ratios, CMC concentration, obstacles geometry, and enclosure size. The heat transfer performance shows the improvement by rising the Ra and CMC % for Cuboid obstacle. The cylindrical obstacle shows the different behavior in which the relation between viscous and buoyant forces is discussed. The optimum heat transfer improvement of 86 % is observed when a cylindrical obstacle is utilized with 1 % CMC. The three-dimensional free convection simulation results have a good agreement with experimental investigation of previous work from the literature.

keywords: *CFD, Natural convection, Non- Newtonian fluid, CMC, obstacle.*

1. Introduction

Natural convection is usually the most important mechanism for heat transfer in closed cavities, have several applications across a wide range of technical systems. The fluids within the cavities are either Newtonian or non-Newtonian as found in many natural or artificial systems. Nanofluids, paints, molten polymers, inks, foodstuffs, organic materials, Non-Newtonian behavior in adhesives, and other materials are common that can be used in electronic cooling systems, food processing, geophysical systems, petroleum exploration, nuclear reactors, and polymer engineering, among other applications. One of the motivations for investigating stratigraphic convection with non-Newtonian fluids like pseudo and dilated plastic fluids is their distinctive and distinct performance, and there are a large number of researchers studying containers with different boundaries conditions and different fluids as well, where Kim et al.[1] studied transient convection of a non-Newtonian energy law liquid model in a closed square container where heating is by raising the temperature of the sidewall and cooling by decreasing the temperature of the opposite wall. The result was an increase in the mean Nusselt number with a decrease in the power-law index n for a given set of Ra and Pr values. Lamsaadi et al. [2] investigated stratigraphic convection in a shallow rectangular container filled with a non-Newtonian fluid that was heated from below and cooled from above by subjecting it to a uniform convection flow while its vertical sides were adiabatic. Whereas the result was that the flow system enhances convective heat transfer when the power-law index is low (shear-thinning fluids, $0 < n < 1$) and gives the opposite result when increasing, as in (shear-thickening fluids, $n > 1$). Lamsaadi et al.[3] also performed a two-dimensional numerical and analytical simulation of a shallow rectangular container, the long horizontal

walls of which are insulated, while the short vertical walls were subjected to a uniform heat flow, filled with non-Newtonian fluids.The results show that the convective values in shallow cavities are affected by the power-law index and Rayleigh number because the shear-thinning behavior ($0 < n < 1$) is enhanced by fluid circulation and convective heat transfer, while the shear is enhanced by the thickening behavior ($n > 1$) resulting in an opposite effect. While Turan et al.[4] studied the natural stratified convection of vertically-walled square containers heated differently, with a Bingham model. The impact of heat and momentum transmission is being investigated for the values of the variables Rayleigh number Ra with ranges (10^3-10^6), Prandtl number Pr (0.1-100), and different ranges of Bingham number, for non-Newtonian and Newtonian fluids, the mean Nesselt number increases as the Rayleigh number increased. But in [5] performed a 2-D numerical simulation of stratified convection in a square-shaped container, but this time using a power-law model. Using lateral heating at a constant temperature with insulated horizontal walls, the effect of force law coefficient in the range (0.6-1.4) on heat transfer and momentum was studied. Both Newtonian and power-law fluids exhibited an increase in the mean Nusselt number as the Rayleigh number increased, and with an increase in shear thickness (i.e. $n > 1$), the average Nusselt number stabilizing in unity (Nu = 1: 0) as the transition occurs Heat is mainly due to thermal conductivity. Pandey et al.[6], Examined the unstable natural convection of a square enclosure containing an inner circular cylinder filled with a non-Newtonian shear-thinning fluid (pseudoplastic) and (expanding) shear thickness fluid (power-law model). The results showed the vertical movement of the inner cylinder and its effect on the heat transfer and flow mechanism inside the container, and under the shear-thinning system, the flux changes into an unstable condition when $n = 0.6$. The rate of heat transmission within the cylinder rises when the container is full of a pseudoplastic fluid (n=1), but it decreases when the enclosure is filled with an expanding fluid ($n > 1$), relative to the Newtonian fluid ($n = 1$). The cylinder surface is subjected to active shear stress as a result of the active shear stress, the Nesselt number falls as the energy law is increased, especially for larger Rayleigh numbers. They also studied the effect of aspect ratio, where Yigit et al.[7] examined and analyzed the Rayleigh-Benard convection and the effect of aspect ratio on it, for non-Newtonian fluids that were represented by an energy law model in a rectangular container with horizontal walls heated with constant temperatures where the lower wall has a higher temperature. The results showed that the convection was weak with an increasing AR aspect ratio. The shape of the flow changed dramatically as the AR changed decreasing (increase) in (Ra, n) values. Lei Wang et al.[8] theoretically studied the effect of the temperature-dependent properties of water-based Nanofluids and their effect on natural convection in a partially heated cubic-shaped container. Nanofluid is used as water and Al2O3 nanoparticles. The temperature field and fluid flow were examined within a temperature difference equal to ($10\ K \leq \_T \leq 50\ K$), with a cold side temperature ranging ($315\ K \leq Tc \leq 335\ K$) and the aspect ratio ($0.5 \leq AR \leq 1$). The heat transfer increase is discovered to be, and the average Nesselt number decrease as the aspect ratio is increased, as well as a reduction in the number of Rayleighs with increasing the size of the nanoparticles the average number of Nesselt decreases. They also studied the location and number of obstacles in closed cavities on the heat transfer effect where, Raisi [9], studied the Natural convection is a cooling method that uses a heat source at the cavity's base to achieve a homogenous heat flux, while the rest of the base was isolated with the side walls, relative to the upper wall at a lower temperature. The results

showed that when increasing the Rayleigh number, the thermal performance increases, especially when the n is less than 1, implying that when shear thinning fluids are used for big Rayleigh numbers, the heat source's cooling effectiveness increases. Mohebbi et al., [10] Natural convection was examined in a closed L-shaped container containing a hot rectangular obstacle and was filled with Nano fluid (Al_2O3/H_2O) with a range of several variables namely Rayleigh number (10^3-10^6), solid volume fraction of the Nanofluid (0-0.05), aspect ratio (0.2- 0.6) as well as examining the effect of the height and location of the obstacle. His showed the average number of Nusselt will increase with increasing Rayleigh number and increasing the concentration of nanoparticles, as well as a decrease in the aspect ratio of the container and an increase in the height of the obstacle. The heat transfer rate is influenced by the location of the obstacle, as it is when the heater is on the left border the average Nusselt number will be enlarged. Pandey et al.[11] also examined the flow and heat transfer properties of a non-Newtonian fluid in a square cavity contain an inner cylinder, as it changed the cylinder's position along its horizontal and diagonal axes in various locations and demonstrated the effect of the behavior of shear-thinning and on the heat transmission mechanism, thickening fluids. The results showed an increase in the rate of heat transfer when using pseudo-plastic fluids, as for the use of dilatant fluids in applications that need a decrease in the rate of heat transfer, the temperature and velocity fields are also affected by the location of the cylinder inside the container, the Nesselt number was also a lowering function of the power law index.

The present work is aimed to simulate heat transfer with natural convection of non-Newtonian fluid inside an enclosure with the hot obstacle by COMSOL Multiphysics. The various parameters are used in the present investigation such as Ra, aspect ratio, obstacle shape, and particles concentrations (CMC). The temperature contours are an important part of the proposed study. The validation analysis with previous investigations is also included.

2. The Numerical Analysis

Figure (1) shows the geometry and coordinate system. The shape is simply represented by a rectangular cavity that is insulated on the sidewalls and has a geometry of a cold top surface at constant temperature and contains an obstacle in the base that is heated at a constant temperature as well. The rest of the base is also thermally insulated. The cavity is filled with a non-Newtonian liquid (carboxymethylcellulose) with different concentrations. The study was carried out for different section lengths.

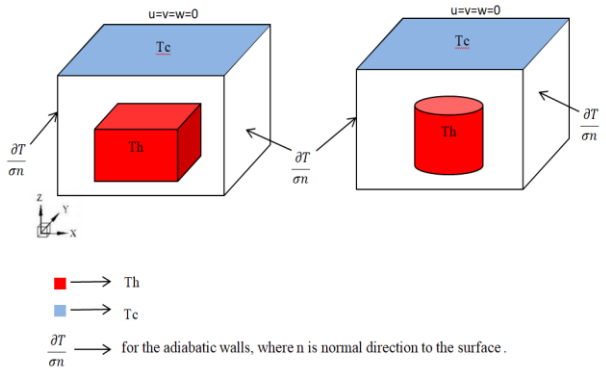

Fig.(1) sketch of the enclosure and coordinates system

2.1 Governing equations

The case is assumed to be filled with a non-Newtonian (power-law) fluid. The fluid flow is laminar, stable, incompressible, three-dimensional, single-phase, and incompressible. The radiation impacts are minimal, as well as density changes. Based on these stated assumptions, the equations used in the present study are presented in the following expressions [12] :

Continuity equation

$$\frac{\partial u}{\partial x} + \frac{\partial v}{\partial y} + \frac{\partial w}{\partial z} = 0 \qquad \ldots\ldots\ldots\ldots\ldots\ldots \quad (1)$$

Momentum equation

X - Component of the momentum equation:-

$$u\frac{\partial u}{\partial x} + v\frac{\partial u}{\partial y} + w\frac{\partial u}{\partial z} = -\frac{1}{\rho}\frac{\partial p}{\partial x} + \frac{\mu}{\rho}\left(\frac{\partial^2 u}{\partial x^2} + \frac{\partial^2 u}{\partial y^2} + \frac{\partial^2 u}{\partial z^2}\right) \qquad \ldots\ldots\ldots\ldots\ldots \quad (2\text{-a})$$

Y - Component of the momentum equation:-

$$u\frac{\partial v}{\partial x} + v\frac{\partial v}{\partial y} + w\frac{\partial v}{\partial z} = -\frac{1}{\rho}\frac{\partial p}{\partial y} + \frac{\mu}{\rho}\left(\frac{\partial^2 v}{\partial x^2} + \frac{\partial^2 v}{\partial y^2} + \frac{\partial^2 v}{\partial z^2}\right) \qquad \ldots\ldots\ldots\ldots\ldots \quad (2\text{-b})$$

Z - Component of the momentum equation:-

$$u\frac{\partial w}{\partial x} + v\frac{\partial w}{\partial y} + w\frac{\partial w}{\partial z} = -\frac{1}{\rho}\frac{\partial p}{\partial z} + \frac{\mu}{\rho}\left(\frac{\partial^2 w}{\partial x^2} + \frac{\partial^2 w}{\partial y^2} + \frac{\partial^2 w}{\partial z^2}\right) \qquad \ldots\ldots\ldots\ldots\ldots \quad (2\text{-c})$$

Heat equation

$$\frac{\partial T}{\partial t} + u\frac{\partial T}{\partial x} + v\frac{\partial T}{\partial y} + w\frac{\partial T}{\partial z} = \frac{k}{\rho cp}\left(\frac{\partial^2 T}{\partial x^2} + \frac{\partial^2 T}{\partial y^2} + \frac{\partial^2 T}{\partial z^2}\right) \qquad \ldots\ldots\ldots\ldots\ldots \quad (3)$$

2.2 The physical properties of non-Newtonian fluids

The physical properties are taken from experimental tests of resultant fluid and solution. The physical properties (ρ, μ, k, cp) are a function of temperature. The viscosity is the main affected by using

non-Newtonian fluids. The shear stress has a non-linear tendency and the shear rate is the hypothetical approach of non-Newtonian fluids. The power model is validated in COMSOL multi-physics commercial package as follows [13]:

$$\mu = m(\gamma)^{n-1} \quad \ldots\ldots\ldots\ldots\ldots\ldots \quad (4)$$

And

$$\gamma = \max\left(\left(\sqrt{2(grad(U) + grad(U)^T) : (grad(U) + grad(U)^T)}\right)\gamma_{min}\right) \ldots\ldots\ldots (5)$$

Where m is Newtonian viscosity, γ is a shear rate and n is exponent constant. Where n=1, the fluid becomes Newtonian. The velocity tensors affect viscosity magnitude and become tensor components when n greater or less than unity.

The boundary conditions of momentum transport are zero pressure at the top of the outer rectangular enclosure and the gravity for the whole enclosure. The heat transfer boundary conditions are the hot surface and Tc at the cold surface (the upper wall of the enclosure). T_h is the hot temperature and T_f is the appropriate fluid temperature.

The average heat transfer coefficient can be obtained by using the integral averaged method as follows [14] :

$$\bar{h} = \frac{1}{v}\int_0^v \frac{q}{T_h - Tf}\, dv \quad \ldots\ldots\ldots\ldots\ldots\ldots \quad (6)$$

Where v is the volume between the inner part and outer part of the enclosure, T_h is the hot temperature and T_f is the appropriate fluid temperature. The volume-averaged heat transfer coefficient is determined by COMSOL software because the T is the magnitude quantity of present work. The averaged coefficient of heat transfer is easily used to find the Nusslt number without going towards the complexity of pictorial quantities. In the present study, the number of Nusselt Nu is provided by [4] :

$$\text{Nu} = \frac{h.l}{k} \quad \ldots\ldots\ldots\ldots\ldots\ldots\ldots \quad (7)$$

where Nu: is the heat transfer rate by convection divided by the heat transfer rate by conduction in the fluid. The Rayleigh number Ra, which is specified in the current study as the ratio of the strengths of thermal transports due to to buoyancy to thermal diffusion, has the following definition: [13]:

$$Ra = \frac{\rho^2.cp.\beta\ .g\ .l^3.(T_H - T_C)}{\mu.k} = \text{Gr Pr} \quad \ldots\ldots\ldots\ldots\ldots\ldots\ldots \quad (8)$$

Where Gr: is the Grashof number and Pr is the Prandtl number, which is defined as :

$$\text{Gr} = \frac{\rho^2.cp.\beta\ .g\ .l^3.(T_H - T_C)}{\mu^2} \quad \ldots\ldots\ldots\ldots\ldots\ldots \quad (9)$$

$$Pr = \frac{\mu Cp}{k} \quad \ldots\ldots\ldots\ldots\ldots\ldots\ldots \quad (10)$$

The Grashof number is the ratio of buoyant and viscous force strengths, whereas the Prandtl number is the ratio of momentum diffusion to thermal diffusion. Because they incorporate the constant plastic viscosity, these definitions are referred to as "nominal" values.

2.3 *Mesh generation and the grid-independent test*

There are many types of mesh, such as Extremely coarse, Extra coarse, coarse, coarser, normal, and fine mesh. Choosing the type of mesh depended on several factors, such as the system geometry, the type of flow. In this study, the number of the element are considered (85979), the number of edge elements (441), the boundary element (7994) as well as the number of the vortex elements (16) at AR=0.5 rectangular obstacle. Given that the discretization grid is triangular, unstructured, and non-uniform as shown in Figure (2). All the numbers of elements gave almost identical results for the Nusselt number so determined as illustrated in Table(1). Ultimately, a mesh number of (85979) was used in this part as this represented the best compromise in terms of both accuracy and computational time. The following equation was used to calculate the relative inaccuracy of the desired parameters [15]**.**

$$Error\% = \frac{|Anew - Aold|}{Anew} \times 100 \qquad \text{..... (11)}$$

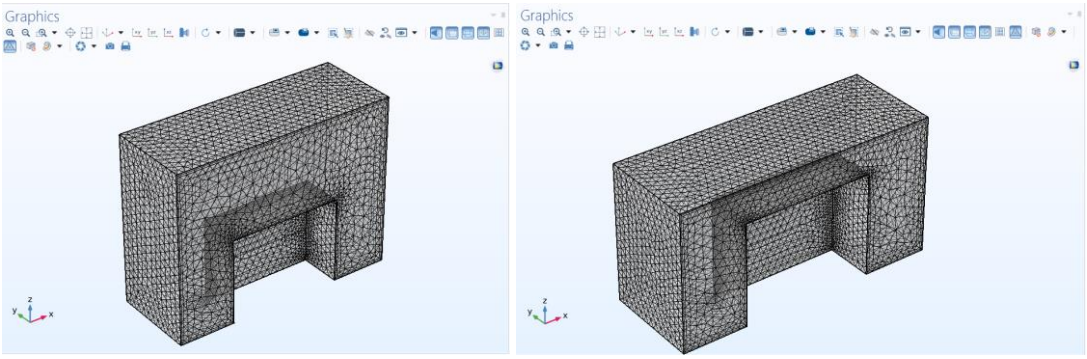

AR=0.5 AR=0.75

Fig. (2) mesh analysis of cuboid obstacle

Where (A) denotes any parameter, including Nusselt number, coefficient heat transfer, temperature, and parameter values obtained from the best grids. As shown in Table (1), a "fine" network gives the lowest error rate, indicating that the network's independence is preserved but with a very long time and requires high specifications.

Table (1) Type of element size and appearance the Average Nusselt number

Mesh size	Number of vortex element	Number of edge element	Number of boundary element	Number of element	Nu	error%
Extra croase	16	236	2536	17163	27.7451	….
coarser	16	298	3932	34156	29.7376	6.7%

coarse	16	441	7994	85979	31.6694	6.09%
normal	16	559	12420	164160	32.6758	3.07%
fine	16	792	23974	398767	32.7445	0.209%

3. Numerical method and model validation

In the current work, for the first time, the COMSOL 5.5 Multiphysics software was utilized to do simulations and In a rectangular enclosure, the three-dimensional fluid and heat transport problem was addressed. Several engineering applications use the computational Fluid Mechanics (CFD) module to study the fluid's behavior and heat transport in different phenomena. CFD module's 10 comprehensive competencies comprise steady and unsteady fluid and two- and three-dimensional heat transfer issues. COMSOL Multiphysics has a CFD module that uses the finite element method to solve the partial differential equations that control the problem domain (momentum, continuity, and energy for two domains solid and fluid). The momentum transport and heat transport equation is used. The partial differential equations (PDEs) of the present system are complex, the finite element method converts these equations into an algebraic matrix depending upon boundary conditions and mesh distribution. The algebraic equations of momentum transport are solved first at the initial temperature, then the resultant velocity profile is introduced to the heat transfer equation in convection term, the resultant temperature distribution is used to estimate the physical properties of momentum and heat transport, then the momentum transport equation is solved again in new temperature distribution and so on. The trial solution of these equations is achieved when the error of tolerance reaches 0.1 % and the convergence is reached. To ensure that numerical findings are accurate. Especially because this is the first research to use the COMSOL Multiphasic code, which employs the finite element approach. Two simulation models, it has been compared with previous numerical studies. The verification form was compared to Kefayati [16] for both streamlines, isotherm contours and average Nusselt number .who conducted a numerical study "Simulation of non-Newtonian molten polymer on natural convection in a sinusoidal heated cavity using FDLBM "The file is inserted using ANSYS CFX Limited Size Based Software. Comparison made Figures (3) show a comparison between the current COMSOL simulations with published accounts show a good agreement, between the two approaches.

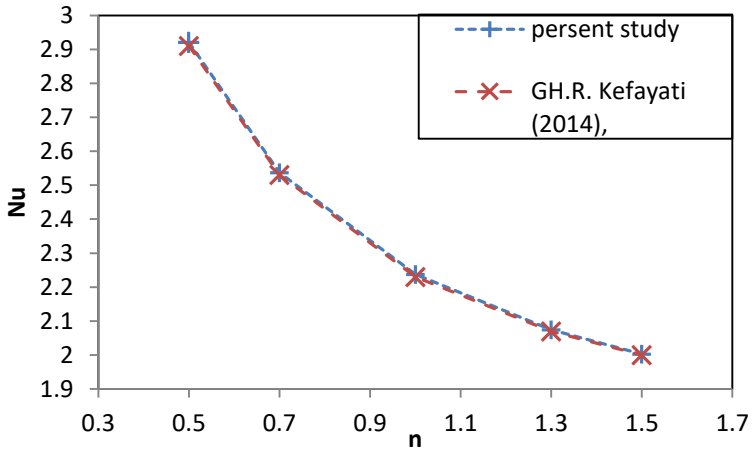

Fig.(3) The average Nusselt number for several power-law indices is compared. & Ra=104 between the present work and GH.R. Kefayati,[16]**.**

4. Results and Discussion

The results of the current study show in the model the effects of Rayleigh number depending on the temperature difference between hot and cold surfaces (5 ° C, 15° C, 25 ° C), and AR (0.5, 0.75). The index power law (0.59, 0.72, 1) according to the CMC polymer concentration in the base fluid (water), the heat source with two different shapes (cylindrical and cuboid) is installed in the same place in the center of the base. Where the results will be discussed for all these variables on the heat transfer inside the enclosure by natural convection. The velocity distribution, temperature distribution, heat transfer coefficient distribution, and streamlines are obtained by applying the simulation. The results are considered the indications of heat transfer mechanisms interaction within the enclosure for various parameters.

4.1 Temperature distribution

Since the obstacle is heated so the heat is transferred from the obstacle into the fluid. Hot fluid around the obstacle exhibits buoyancy forces and starts to rise against gravity and the temperature distribution depends upon the heat transfer physics configuration and momentum transport results in convection terms. The differences are more visible, especially at the top of the obstacle. Figure (4) show the temperature distribution for various CMC content (n value as Non-Newtonian fluid indication), for a cuboid shape of the obstacle. The increasing of hot temperature Th or Ra (by increasing temperature difference) increases the temperature range inside the enclosure. The increasing of n lowers the heat transfer tendency, the results show the hot fluid particles migrates upward direction parallel to gravity action, the higher Ra means a higher volume of migrated fluid by gravity forces or density difference. As the Rayleigh number rises, so does the intensity of the rotating buoyancy force. The biggest improvement in convection intensity occurred at n = 0.59 because shear-thinning fluids have a lower apparent viscosity than Newtonian fluids. The effect of CMC % appears directly upon the physical properties (viscosity, density, and thermal conductivity are a function of temperature). The decreasing (n) as explained before rises are corrected by the shear stress correction factor according to power law

which is affected by velocity components. The velocity components are resulted due to momentum conservation. The correction factor of non-Newtonian fluid acts as braking forces to Newtonian behavior. In other words, the decreasing of temperature promotes the increasing of viscosity for Newtonian fluid whereas the shear stress which is powered to (n) (non- Newtonian exponent term) reduces the action of viscosity action. For various obstacle shapes and AR, the decreasing of n dissipates the temperature be for a wider area at lower temperature with low gradient tendency. The higher temperature shows sharp behavior toward the index power-law value.

Water (n=1) 0.5 % CMC (n=0.729) 1 % CMC (n=0.59)

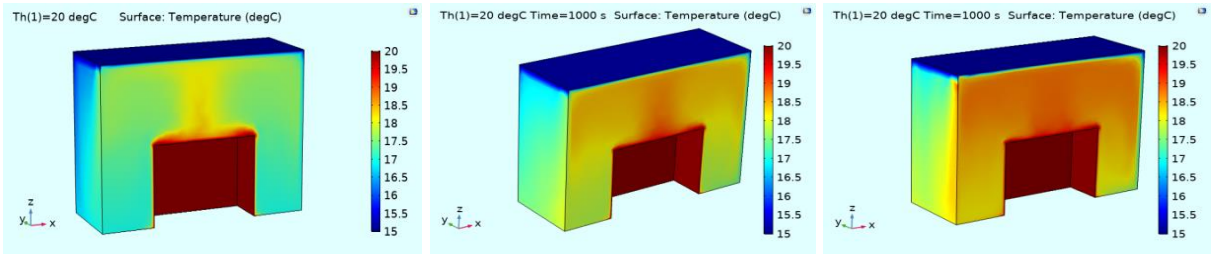

Ra= 2.13 x10^6, Th= 20 ◦C

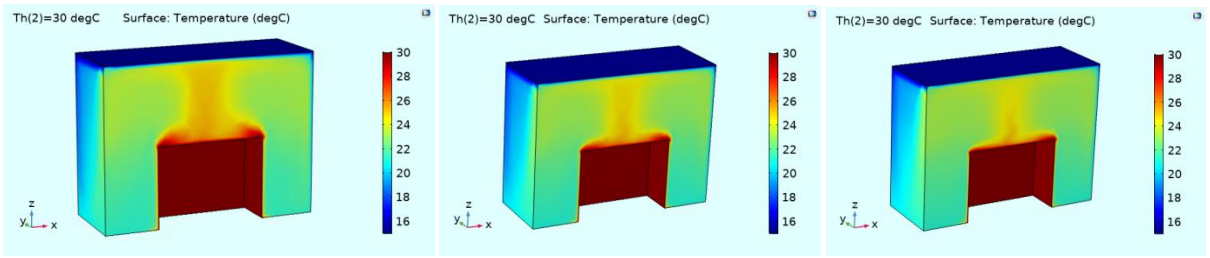

Ra= 6.38 x10^6, Th=30 ◦C

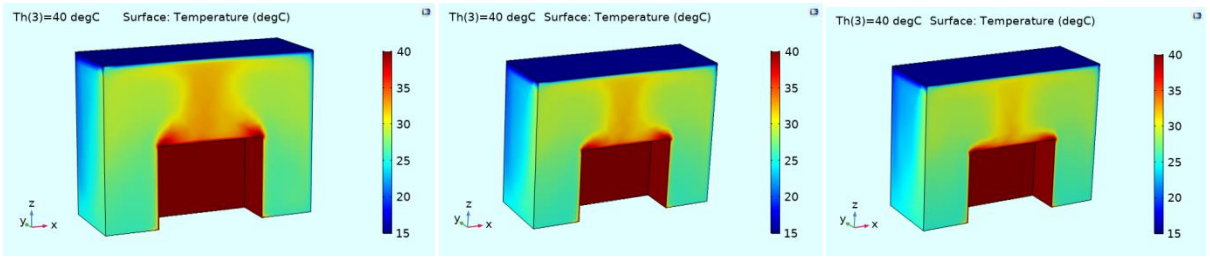

Ra= 1.06 x10^7, Th= 40 ◦C

Fig. (4) Temperature distribution of water, 0.5 % CMC and 1 % CMC inside a cuboid obstacle of AR=0.5 for various Ra and Th.

Figure (5) indicates the effect of the AR of a cuboid obstacle on temperature distribution. The dispersion of heat transfer when AR=0.75 is not regular natural convection comparing with AR=0.5, in space between the enclosure and obstacle because of the boundary layers interactions and the conductive heat transfer tendency. The increasing temperature difference rises the natural convection action and reduces the conductive heat transfer.

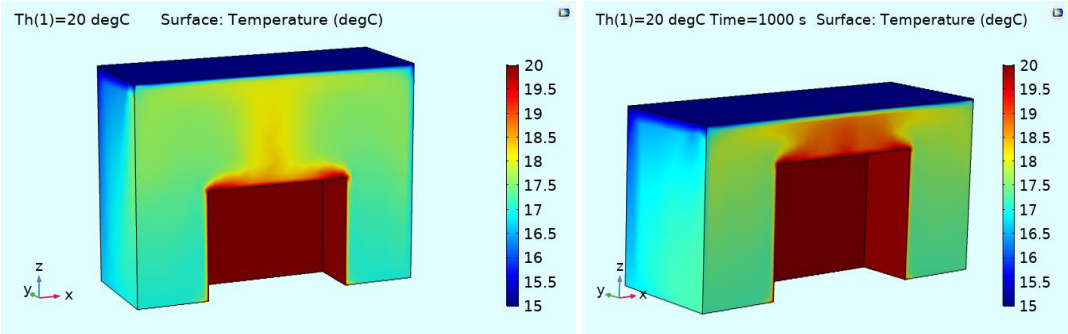

Ra= 2.13 x10^6,Th= 20 ◦C

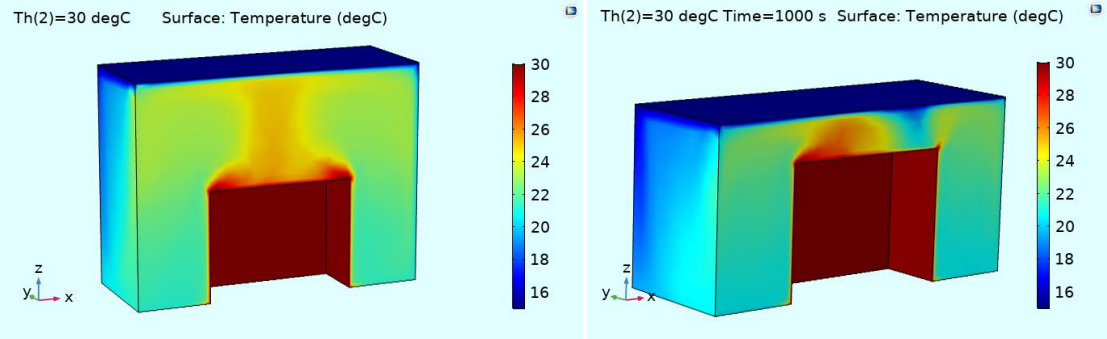

Ra= 6.38 x10^6, Th=30 ◦C

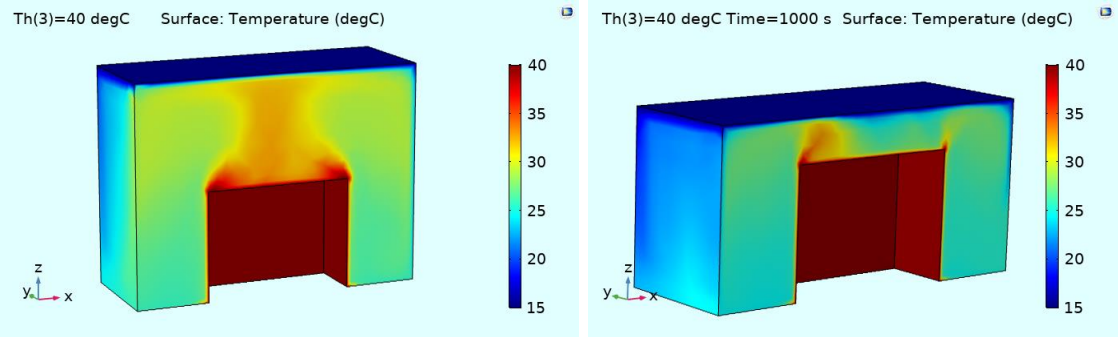

Ra= 1.06 x10^7,Th= 40 ◦C

Fig. (5) Temperature distribution inside a cuboid obstacle of AR=0.5 and 0.75 for various Th.

Figures (6) and (7) show the effect of obstacle shape on temperature distribution for various AR and Th. The curvature area of hot particles migration upwards appears for a cylindrical obstacle in general cases. At AR=0.5 the migration rate seemed to be equal with the maximum behavior of heat transfer natural convection in cuboid case. The cuboid hot surface area in a perpendicular direction to gravity action is higher than the cylinder case. For AR=0.75, the conductive heat transfer mechanisms are seemed to be the major control mechanism within the system because of the short distance between the two surfaces of the enclosure.

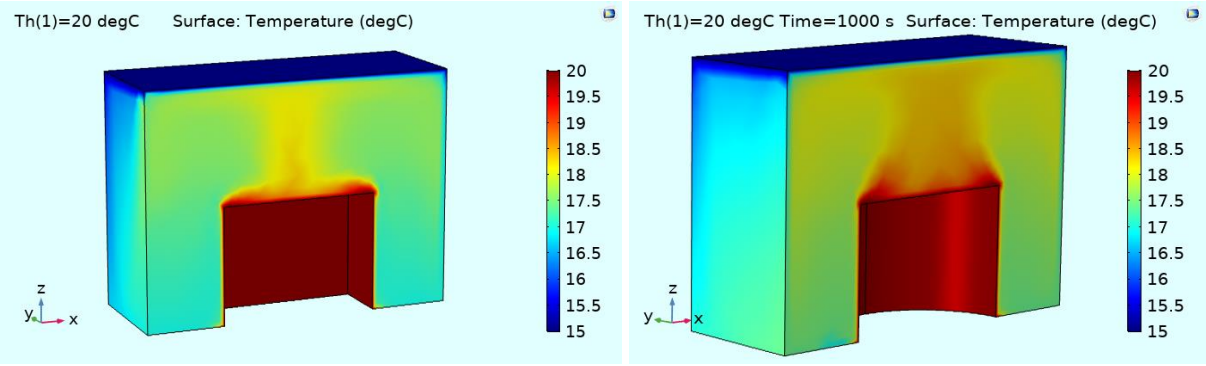

Ra= 2.13 x10^6,Th= 20 ◦C

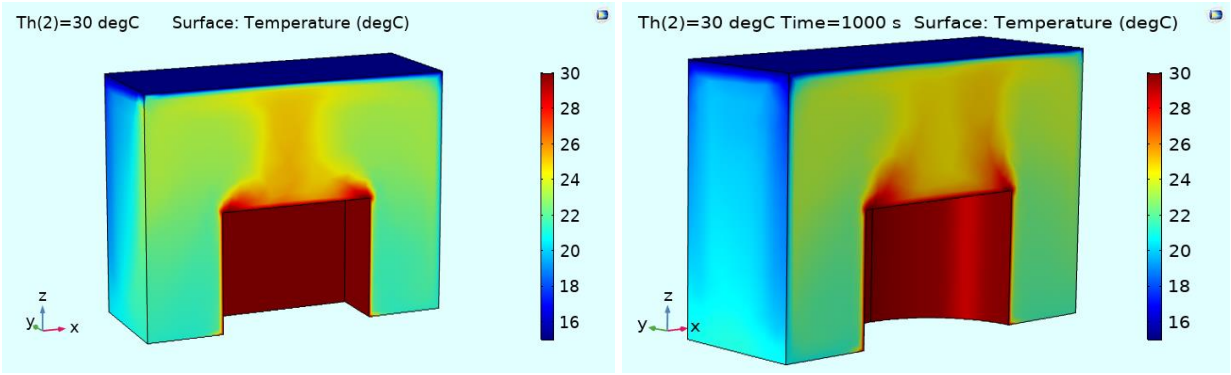

Ra= 6.38 x10^6, Th=30 ◦C

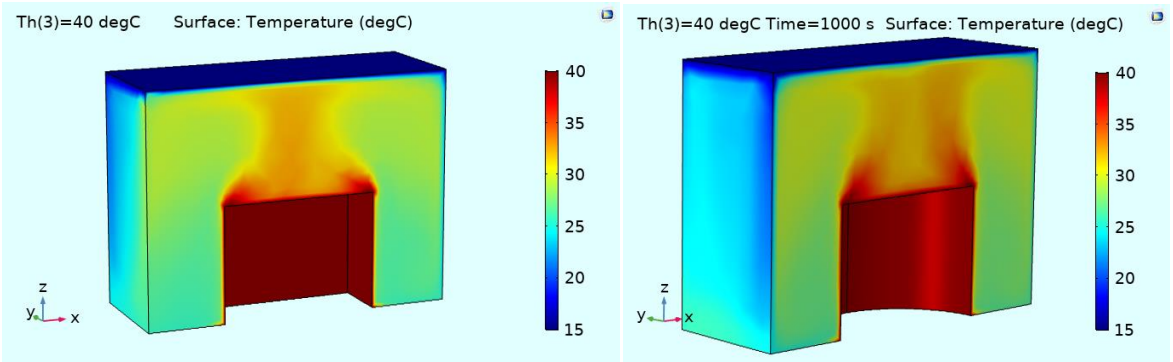

Ra= 1.06 x10^7,Th= 40 ◦C

Fig. (6) Temperature distribution water inside cuboid and cylindrical obstacle of AR=0.5 for various Th.

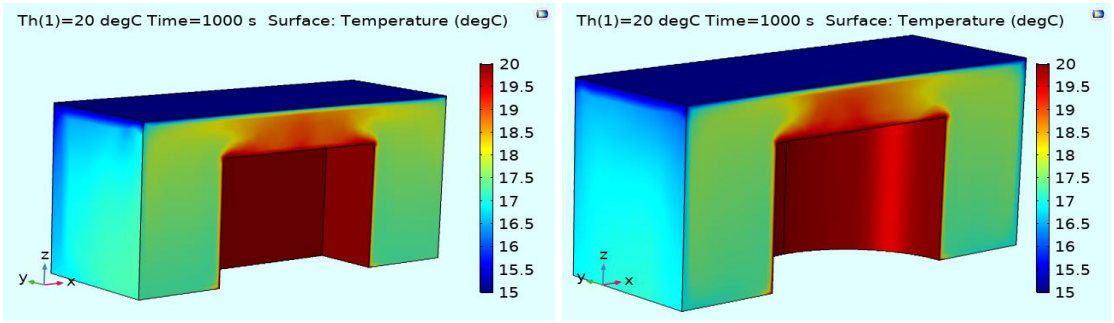

Ra= 2.13 x10^6,Th= 20 ◦C

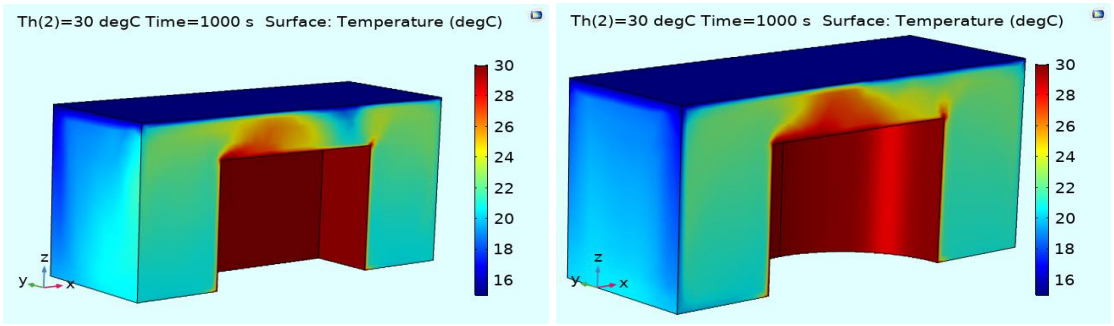

Ra= 6.38 x10^6, Th=30 ◦C

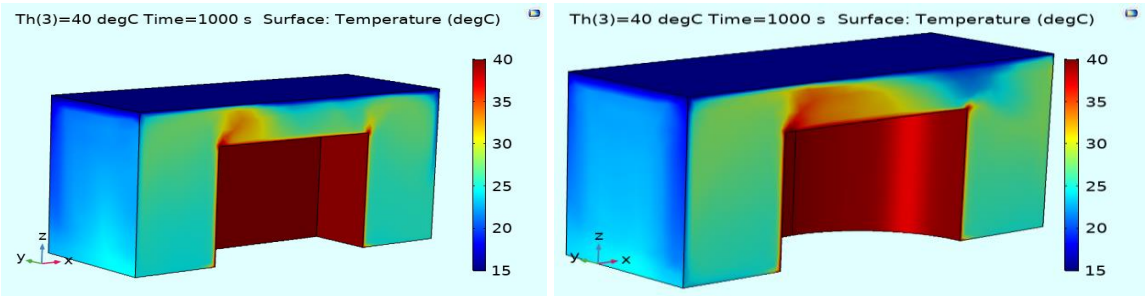

Ra= 1.06 x10^7,Th= 40 ◦C

Fig. (7) Temperature distribution inside cuboid and cylindrical obstacle of AR=0.75 for various Th.

4.2 Heat transfer coefficient

The heat transfer coefficient is determined by applying equation (7) for the whole enclosure. Figures (8) to (11) show the Nu vs. Ra plots for various AR, CMC %, and obstacle shapes. The non-direct proportional between the Ra and Nu is shown for CMC content and AR=0.75, while the water case shows linear behavior of Ra on Nu. The non-Newtonian fluids have dependent on temperature, so the nonlinear behavior is converted into polynomial behavior. For the AR effect, the thermal boundary layers of two surfaces will be interacted by increasing AR in addition to decreasing the gravity momentum region by decreasing the distance. The cylinder shape has nonuniform temperature distribution, so the hot fluid particles will be slightly minimum values and have non-regular polynomial

Nu vs. Ra trends. The heat transfer coefficient decreases by increasing n (increasing CMC %) but the general case of Nu is reverse to heat transfer coefficient because the deducing in heat transfer coefficient ratio is less than thermal conductivity reduction. The maximum heat transfer increasing is 86 % by utilizing 1 % CMC for a high Ra value.

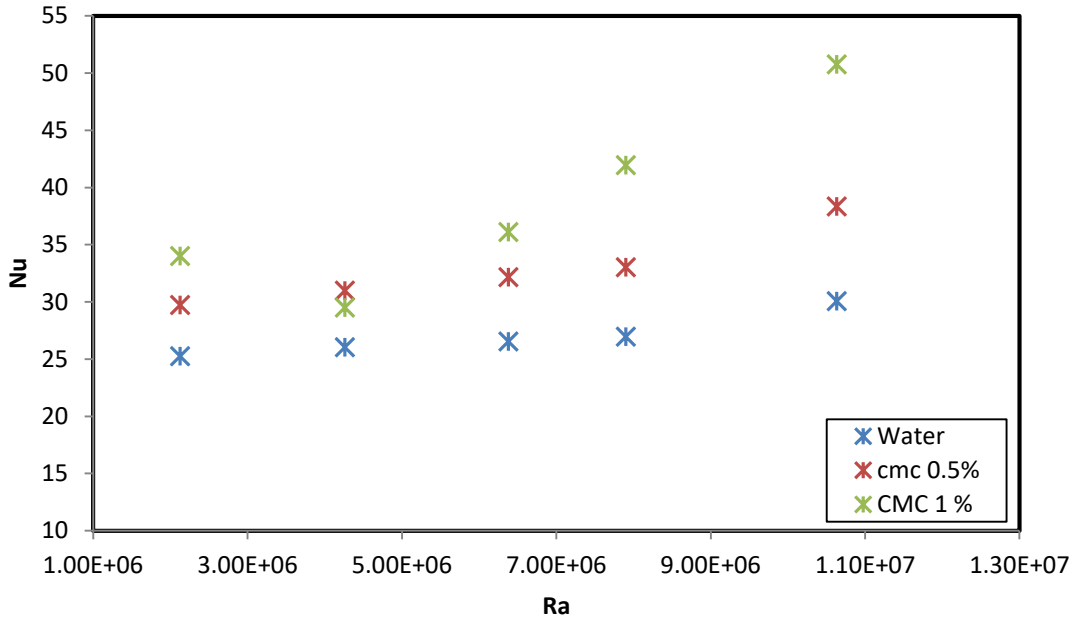

Fig.(8) Nu & Ra plots for various CMC % for rectangle obstacle , AR=0.5

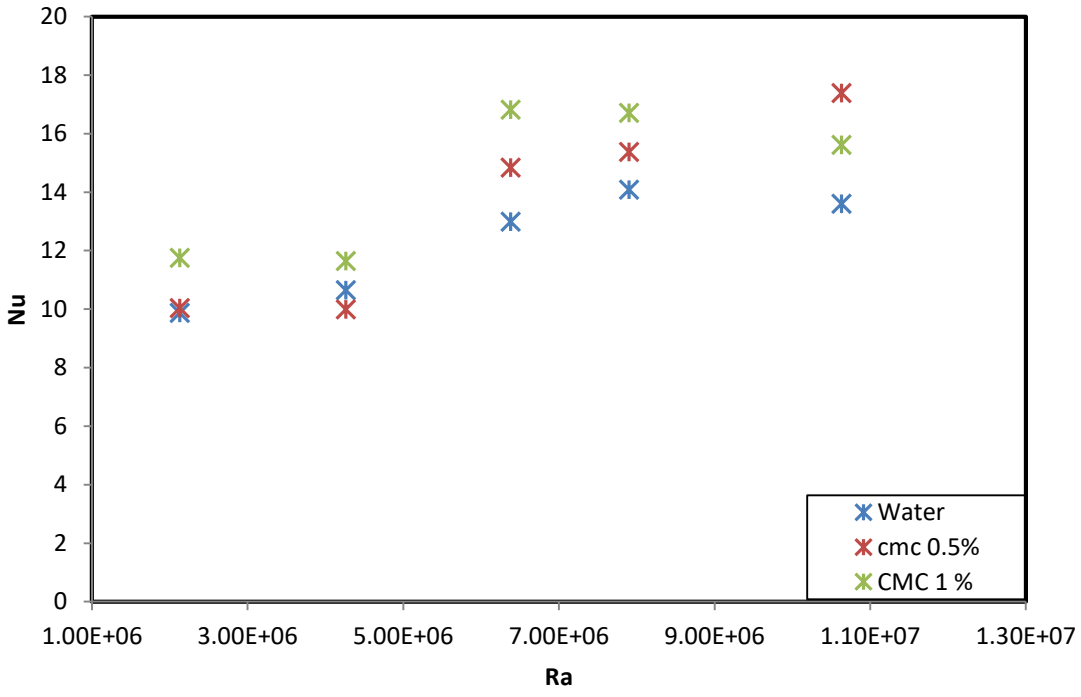

Fig. (9) Nu & Ra plots for various CMC % for rectangle obstacle , AR=0.75

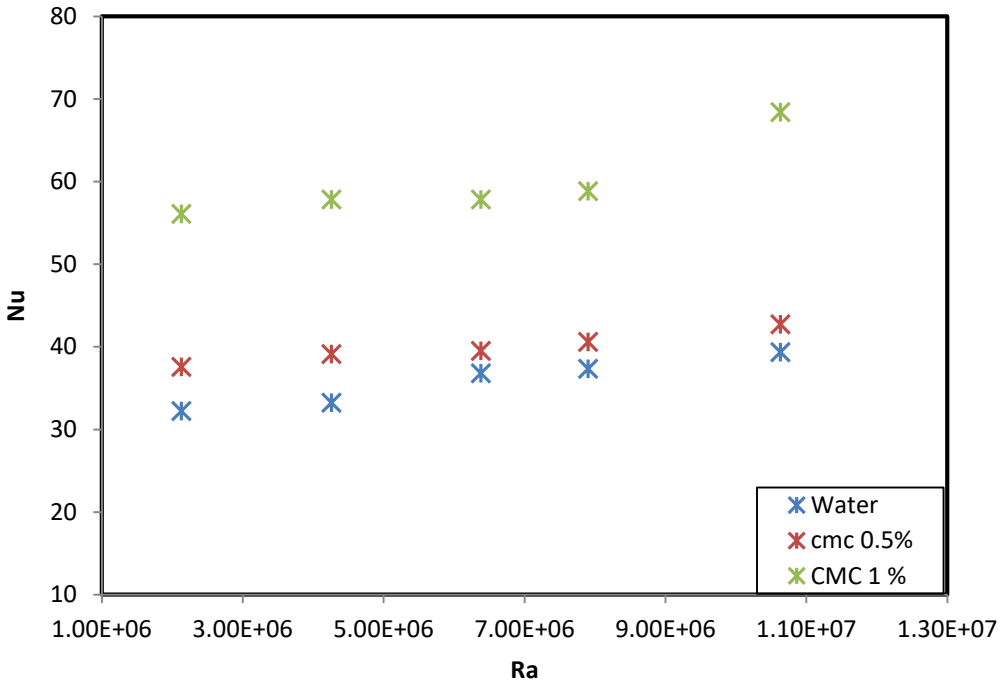

Fig. (10) Nu & Ra plots for various CMC % for cylindrical obstacle , AR=0. 5

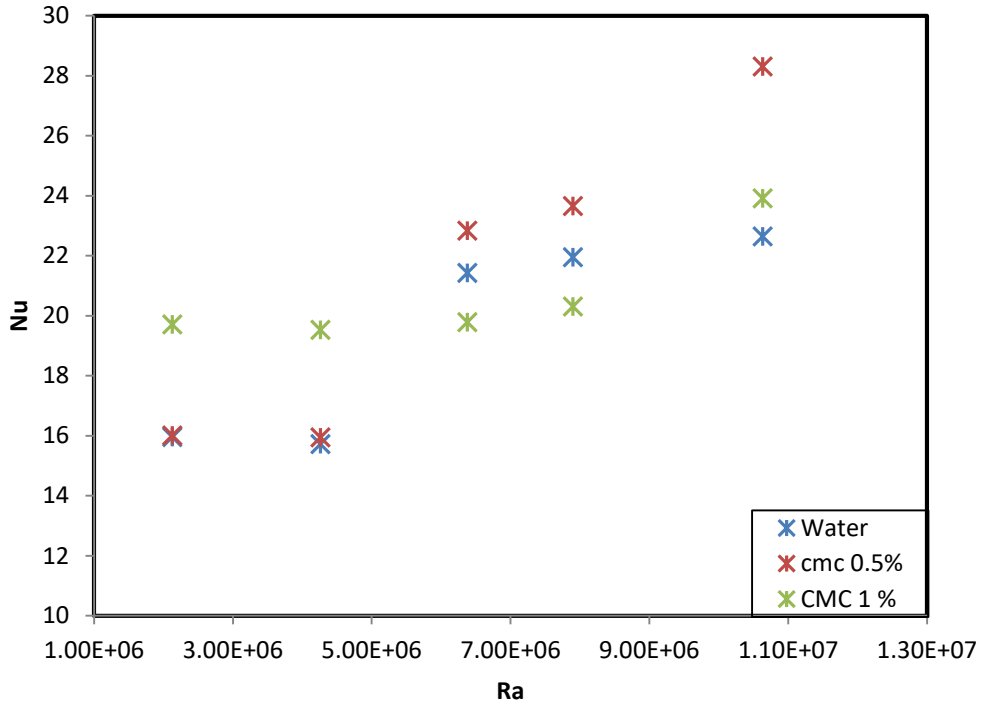

Fig. (11)Nu & Ra plots for various CMC % for cylindrical obstacle , AR=0.75

5. conclusions

The heat transfer free convection has been validated and simulated accurately for rectangular enclosures with ostriches of various shapes. The relation between the various parameters (% CMC, AR, geometry, and Ra) with Nu is exhibited through the present study. The effect of CMC % has alerted the heat transfer behavior by changing the n (exponent of the viscosity power-law for non-Newtonian fluid). The maximum heat transfer improvement of about 86 % results from the investigation. The temperature contours show the turbulent tendency of free convection when the lower value of n indicates the law molecular values of heat transfer and momentum transport. The lower thermal conductivity of CMC % with high shear stress due to viscous power-law action through free convection indicates the unusual behavior of a present system.

Nomenclature

Symbols	Notations	units
h	heat transfer coefficient	$W/m^2.K$
Nu	Nusselt number	-
T	Temperature	◦C
q	heat flux	w/m^2
A	Surface area	m^2
cp	Heat capacity	J/Kg. K
K	Thermal conductivity	W/m. K
g	gravity acceleration	m/s^2
Gr	Grashof number	-
Ra	Rayleigh number	-
Pr	Prandtl number	-
AR	Aspect ratio = $\frac{l}{H}$	-
l	The characteristic length which length between hot and cold walls	m
H	height of enclosure	m
u, v, w	velocity components in the x- ,y- and z-direction, respectively	m/s
n	a dimensionless constant called the power-law index	
m	the consistency factor, which is an indicator of the degree of the fluid viscosity	

Greek letters

Symbol	meaning	units
μ	Dynamic viscosity	kg/m. s
β	thermal expansively	K^{-1}
ρ	Density	kg/m^3
γ	shear rate	

Subscribes

h	hot
c	cold

Abbreviations

CFD	Computational fluid dynamic

References

[1] G. Bin Kim, J. M. Hyun, and H. S. Kwak, "Transient buoyant convection of a power-law non-Newtonian fluid in an enclosure," *Int. J. Heat Mass Transf.*, vol. 46, no. 19, pp. 3605–3617, 2003, doi: 10.1016/S0017-9310(03)00149-2.

[2] M. Lamsaadi, M. Naïmi, and M. Hasnaoui, "Natural convection of non-Newtonian power-law fluids in a shallow horizontal rectangular cavity uniformly heated from below," *Heat Mass Transf. und Stoffuebertragung*, vol. 41, no. 3, pp. 239–249, 2005, doi: 10.1007/s00231-004-0530-8.

[3] M. Lamsaadi, M. Naïmi, and M. Hasnaoui, "Natural convection heat transfer in shallow horizontal rectangular enclosures uniformly heated from the side and filled with non-Newtonian power-law fluids," *Energy Convers. Manag.*, vol. 47, no. 15–16, pp. 2535–2551, 2006, doi: 10.1016/j.enconman.2005.10.028.

[4] O. Turan, N. Chakraborty, and R. J. Poole, "Laminar natural convection of Bingham fluids in a square enclosure with differentially heated side walls," *J. Nonnewton. Fluid Mech.*, vol. 165, no. 15–16, pp. 901–913, 2010, doi: 10.1016/j.jnnfm.2010.04.013.

[5] O. Turan, A. Sachdeva, N. Chakraborty, and R. J. Poole, "Laminar natural convection of power-law fluids in a square enclosure with differentially heated side walls subjected to constant temperatures," *J. Nonnewton. Fluid Mech.*, vol. 166, no. 17–18, pp. 1049–1063, 2011, doi: 10.1016/j.jnnfm.2011.06.003.

[6] S. Pandey, Y. G. Park, and M. Y. Ha, "Unsteady analysis of natural convection in a square enclosure filled with non-Newtonian fluid containing an internal cylinder," *Numer. Heat Transf. Part B Fundam.*, vol. 77, no. 1, pp. 1–21, 2020, doi: 10.1080/10407790.2019.1685838.

[7] S. Yigit, R. J. Poole, and N. Chakraborty, "Effects of aspect ratio on laminar Rayleigh-Bénard convection of power-law fluids in rectangular enclosures: A numerical investigation," *Int. J. Heat Mass Transf.*, vol. 91, pp. 1292–1307, 2015, doi: 10.1016/j.ijheatmasstransfer.2015.08.032.
[8] L. Wang, B. Shi, and Z. Chai, "Effects of temperature-dependent properties on natural convection of nanofluids in a partially heated cubic enclosure," *Appl. Therm. Eng.*, vol. 128, pp. 204–213, 2018, doi: 10.1016/j.applthermaleng.2017.09.006.
[9] A. Raisi, "Natural convection of non-Newtonian fluids in a square cavity with a localized heat source," *Stroj. Vestnik/Journal Mech. Eng.*, vol. 62, no. 10, pp. 553–564, 2016, doi: 10.5545/sv-jme.2015.3218.
[10] R. Mohebbi, M. Izadi, H. Sajjadi, A. A. Delouei, and M. A. Sheremet, "Examining of nanofluid natural convection heat transfer in a Γ-shaped enclosure including a rectangular hot obstacle using the lattice Boltzmann method," *Phys. A Stat. Mech. its Appl.*, vol. 526, p. 120831, 2019, doi: 10.1016/j.physa.2019.04.067.
[11] S. Pandey, Y. G. Park, and M. Y. Ha, "Flow and heat transfer characteristics of the non-Newtonian fluid in a square enclosure containing an internal cylinder," vol. 34, no. 7, pp. 1–16, 2020, doi: 10.1007/s12206-020-0639-9.
[12] F. T. U. L. Koabra, "Study of Natural Convective Heat Transfer of Nanofluids in Cubical Enclosure," 2016.
[13] F. H. Ali, H. K. Hamzah, K. Egab, M. Arıcı, and A. Shahsavar, "Non-Newtonian nanofluid natural convection in a U-shaped cavity under magnetic field," *Int. J. Mech. Sci.*, vol. 186, p. 105887, 2020, doi: 10.1016/j.ijmecsci.2020.105887.
[14] L. Khezzar, D. Siginer, and I. Vinogradov, "Natural convection of power-law fluids in inclined cavities," *Int. J. Therm. Sci.*, vol. 53, pp. 8–17, 2012, doi: 10.1016/j.ijthermalsci.2011.10.020.
[15] N. M. Muhammad, N. A. C. Sidik, A. Saat, and B. Abdullahi, "Effect of nanofluids on heat transfer and pressure drop characteristics of a diverging-converging mini channel heat sink," *CFD Lett.*, vol. 11, no. 4, pp. 105–120, 2019.
[16] G. R. Kefayati, "Simulation of non-Newtonian molten polymer on natural convection in a sinusoidal heated cavity using FDLBM," *J. Mol. Liq.*, vol. 195, pp. 165–174, 2014, doi: 10.1016/j.molliq.2014.02.031.